Characterizing Strategies of Fixing Full Scale Models in Construction Photogrammetric Surveying

Ryan Hough and Fei Dai

West Virginia University, Department of Civil and Environmental Engineering, P.O. Box 6103, Morgantown, WV 26506-6103; PH (304) 293-9940; FAX (304) 293-7109; email: {rhough@mix.wvu.edu; fei.dai@mail.wvu.edu}

ABSTRACT

In construction photogrammetric surveying, it is imperative to convert the relative scale of a 3D model into absolute measurements so geometric measurements can be taken. Previous work suggests this can be done through the determination of a reference line in absolute units, but the position and quantity of reference lines has not been investigated. This paper attempts to characterize the behavior of different strategies in selecting reference lines. Factors including relative position of the reference line, the number of reference lines, and spatial relationships of the reference lines are considered. Three infrastructure objects serve as the test beds, and experiments using various layouts of scale bars (calibrated reference lines) are conducted on each object. The surveying results are then compared with ground truth data, which allows for accuracy determination and aids in determining the best strategy in selecting reference lines for scale fixing. The results from these experiments show that one horizontal reference line in the middle of the object performed with consistent accuracy, but if a specific area on the object needs more accurate measurements it is best to select a reference line in that area. Using three reference lines is ideal from a time and accuracy improvement perspective.

INTRODUCTION

Photogrammetric surveying has been proven to be an efficient way in various construction applications (e.g., Shufelt 1996; Dai and Lu 2008; Kim and Kano 2008). This technique produces three-dimensional representations of site elements, by which geometric measurements can be taken out of the resulting representations. To enable photogrammetric surveying, a key step is to convert a model from relative to absolute measurements. This can be done through using control points with known absolute coordinates, stereo camera set, GPS/IMU (Global Positioning System/Inertial Measurement Unit), or setting a reference line with a known distance. Among these methods, the most time and cost effective solution is using a reference line with a known distance (Grussenmeyer and Khalil 2002). Despite this, the position, quantity, and spatial relationship of reference lines have not been investigated. Consequently, it is unknown where the source of error comes from in this method.

As a key step in identifying accuracy improvement, this paper is to measure the impacts various scale bar scenarios. The remainder of this paper is organized as

follows: The principles of photogrammetry and current methods of absolute scale setting will be discussed first, the experimental design will be explained, the experimental results will be given, and lastly the conclusions of our research and potential applicability in the construction industry will be discussed. The goal of this task is to perform 3D modeling of building and civil infrastructure objects and characterize strategies of fixing full scale models of these objects. The findings are expected to help better utilize photogrammetry as a cheap, quick and safe solution to taking geometric measurements of large scale construction site components.

CURRENT METHODS IN FIXING FULL SCALE MODELS

The basic equations underlying photogrammetry are Collinearity Equations (Wolf 1983). These equations synchronize the 2D image coordinate system with the object's real-world coordinate system. This is accomplished by relating the interior orientation of the camera to the exterior orientation of the object space. Once the Collinearity Equations are accurately set, the relative orientation of the model can be established. In order to determine accurate measurements and spatial relationships on a given model, the relative orientation must be transformed to an absolute orientation in real-world units. There are several different methods available to do this in various photogrammetry applications.

Control points are widely used for setting the absolute orientation. They are points with known coordinates that can be referenced to set the absolute scale of a model. In aerial photogrammetry surveying, ground control points (GCP), which are identifiable object with a known size, are selected so that the scale of the model can be set in real world units. This method is limited when the terrain is mountainous and covered with foliage and trees and if there is a lack of clear existing usable targets. Also, GCPs are difficult to set in a convenient and computer compatible form (Smith and Park 2013). In general, GCPs are not readily available in most situations, making this method impractical. A method using GPS/IMU can simultaneously measure the full exterior orientation while data is being recorded. This method involves two steps: 1) GPS/IMU pre-processing and 2) pre-determined sensor calibration. In the first step the GPS signal and IMU measurements are transformed into object space coordinates. There are two methods that Wegman (2002) suggests for sensor calibration, a direct or integrated method, both of which requires GPS/IMU observations and ground control information. This method produces precise results for various applications; however, it is not widely available and can be tedious. Using a stereo rig that fixes the baseline of two cameras is another way to enable absolute measurement of an object. This method requires pre-configured camera set and maintaining two cameras' relative position when taking photos in field (Brilakis et al. 2011). As the baseline is known, the relative and absolute orientations can be accomplished simultaneously. The stereo photogrammetry is often used, but extra efforts and time is needed for preparing the rig and camera set.

Out of all the techniques for absolute scale fixing, applying reference lines is chosen in our study because it is most time effective, easy-to-use, and performs with sufficient accuracy for construction applications. Our expectation prior to the experiment was as the number of scale bars increases, so does the level of accuracy.

EXPERIMENTAL DESIGN

The following section describes the design and technical components of the experiment. This process is quantified such that it could easily be implemented by any construction professional that has the necessary equipment.

Calibrating Camera and Lens Parameters. To produce the models for our experiment, two cameras were used: a Canon EOS Rebel T3i and a Canon EOS 60D, and two lenses were used: a Canon EF 35mm and a Canon EF-S 18-135mm. These camera lenses are made up of a combination of lenses all assumed to be collinear. The calibration process corrects the radial and decentralizing lens distortion so that an accurate coordinate system and accurate scales can be established. In our research, we applied a fully-automated process and a self-calibration process in iWitness (Fraser 1997) to ensure any error due to the camera lens would be minimized. iWitness is one of the leading close-range photogrammetry software systems because of its accurate 3D measurements and usability. It was used because of this and the potential for construction professionals to easily adapt to using it.

Photo Taking and Setting Scale Bar Scenarios. After the cameras were calibrated, photos were taken of each object from an evenly distributed quantity of positions and angles around the surrounding area of the object. To ensure accuracy, it is a good practice to cover each point on the object in three or more photos. Red-reflective markers (specifically used in iWitness) were attached to the object so that the relative orientation of the object could be quickly and easily established. This is especially useful when the object being modeled does not have prominent natural features to reference. The photos were also taken while different quantities and locations of scale bars were placed in the scene. This is so the absolute orientation could be established after the marking and referencing process and so that the absolute orientation process could be characterized. The scale bars used in the experiment were finely calibrated to be 30". The six scale bar scenarios are planned as in Figure 1.

Marking Referencing and Setting Scales of Models. Once the photos were taken of each object, they were imported into iWitness. After the camera is adequately calibrated and the project photos are imported, points can be marked and referenced. Point marking and referencing is a process that matches the same points in different photos, taken from different locations and angles, so that the relative orientation of the object can be established. As mentioned earlier, several red reflective markers were taped to the objects so that this process would be accelerated by the automated feature in iWitness. After the relative orientation of the model was established by the marking and referencing process, the absolute orientation was set by referencing the scale bar distance (or distances) to its 30" calibrated length. Once the scale bars are referenced in each model, accuracy comparisons were made on the models.

Accuracy Comparisons. There is a built-in distance function in iWitness that allows the user to measure the distance between two points. After the scale bars were referenced in the photos, twenty or more sample distances were determined so that

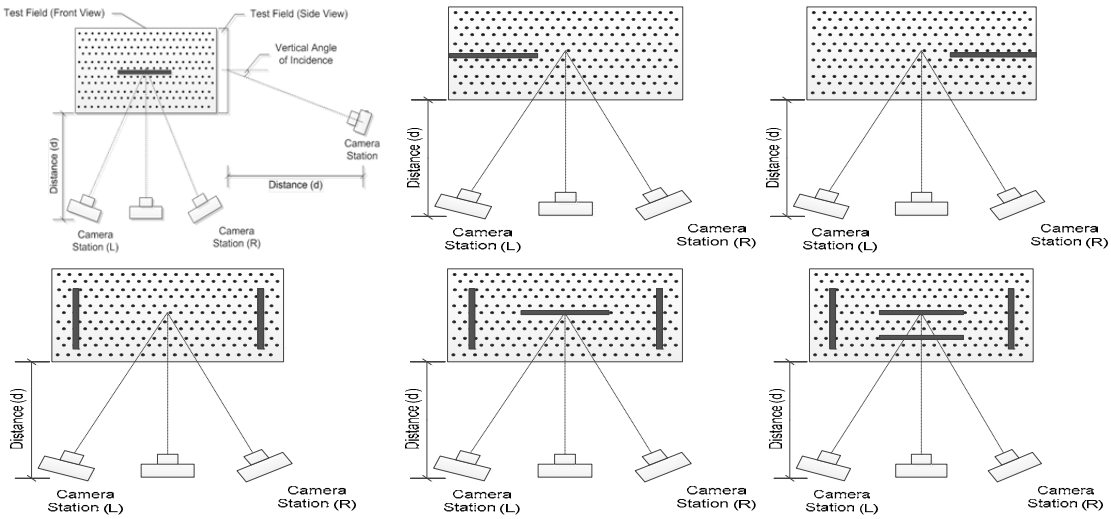

Figure 1. Six Scale Bar Scenarios (from left to right, top down): a) Scenario 1, b) Scenario 2, c) Scenario 3, d) Scenario 4, e) Scenario 5, f) Scenario 6

there would be a significant sample size to do a comparison. The sample distances were collected by a total station or a tape measure and were compared to the distance values given by the iWitness models produced by the six scale bar scenarios. The values were compared to one another in hopes to characterize scale bar placement.

EXPERIMENTAL IMPLEMENTATION AND RESULTS

In implementing the experimental procedure for the selected objects, photos were taken from approximately two meters away. This ensured that a high level of accuracy would be accomplished. The three objects that were modeled were a section of sidewalk, a section of a retaining wall, and a small storage building (Figure 2).

Lastly, Table 1 is a summary table of the parameters from each model. It displays the different camera/lens combinations, the number of pictures, the baseline between consecutive camera stations, the percent coverage which is the overlapped area between two adjacent photos, and the resolution of the pictures.

Figure 2. Left to right: a) Sidewalk slab, b) Retaining wall, c) Storage building

Table 1. Settings of each model.

	Slab Model	Retaining Wall	Full Building
Camera Model	Canon EOS Rebel T3i	Canon EOS 60D	Canon EOS 60D
Lens Model	Canon EF-S 18-135mm	Canon EF 35mm	Canon EF 35mm
# of Photos Taken	82	85	76
Baseline (m)	1	1	1.5
Percent Coverage	50%	58%	43%
Resolution (mp)	18	18	18

Object 1: Sidewalk Slab. The concrete slab model presented a challenge because of its position on the ground and its planar shape. The scale bars were laid directly on the ground in the scenario positions listed above. There were twenty sample distances oriented diagonally, vertically, and horizontally to ensure that accurate comparisons could be accomplished. The ground truth values for this object were collected by a tape measure.

Overall, results from all scenarios are comparable. Scenario 2 performed with the best accuracy results with an average absolute distance of 3.25 mm, an average percent difference value of 0.18%, and a standard deviation of 2.76 mm. Scenario 5 was next best (3.36 mm, 0.18%, and 3.41mm), then Scenario 6 (3.51 mm, 0.19%, and 3.40 mm), Scenario 4 (3.54 mm, 0.19%, and 3.02 mm), Scenario 3 (3.58 mm, 0.19%, and 2.76 mm), and lastly Scenario 1 (4.18 mm, 0.21%, and 3.22 mm). Figure 3 shows a scatter plot of the percent difference values by Scenario. The majority percent differences are within 0.4%.

Object 2: Retaining Wall. The curved shape of the retaining wall presents a difficult task when attempting to produce accurate models. The scale bars were attached to tripods and arranged according to the scenario. Thirty-two sample distances were selected between the red reflective points on the markers attached to the wall and then used for accuracy comparisons. The ground truth data was collected with a tape measure by measuring the distance between the centers of two points on the markers taped to the wall, and there may be some inaccuracy involved because of this.

For the left side, Scenario 2 on average performed with the greatest amount of accuracy with an average absolute difference of 2.29 mm, an average percent difference of 0.16%, and a standard deviation of 1.90 mm. Scenario 1 performed with the next best accuracy (3.67 mm, 0.33%, and 1.85 mm); then Scenario 6 (6.79 mm, 0.58%, and 2.56 mm), Scenario 5 (6.83 mm, 0.59%, and 2.56 mm), Scenario 4 (7.63 mm, 0.65%, and 2.71 mm), and lastly Scenario 3 (9.37 mm, 0.75%, and 3.24 mm). These results are interesting because even though Scenarios 4, 5, and 6 have more scale bars referenced on both sides of the wall, Scenario 1 and 2 still outperformed them. Scenario 2 outperformed Scenario 3 which we expected because Scenario 2 has a scale bar referenced on the left side of the wall. The graph below (Figure 4) shows the percent differences for the left side sample distances of the retaining wall.

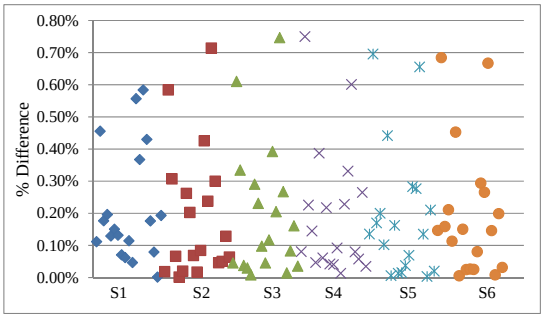

Figure 3. Slab % Differences

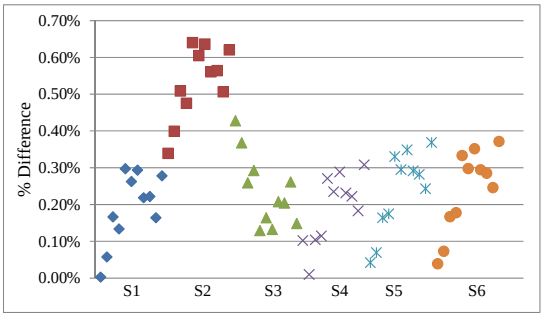

Figure 4. Left side % differences

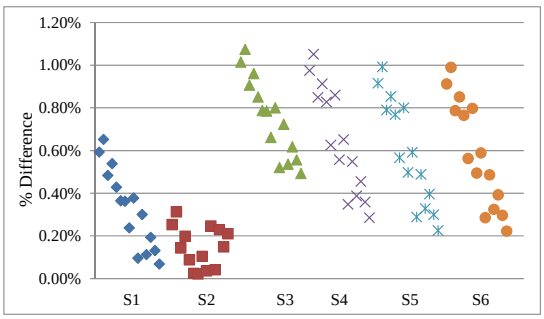

Figure 5. Middle side % differences

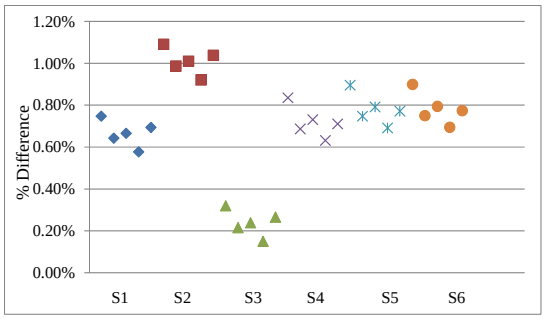

Figure 6. Right side % differences

For the middle section, Scenario 1 (3.60 mm, 0.19%, and 2.26 mm), Scenario 3 (3.49 mm, 0.24%, and 1.34 mm), and Scenario 4 (3.58 mm, 0.19%, and 2.42 mm) performed with the best accuracy. Scenario 5 (4.51 mm, 0.24%, and 2.91 mm) and Scenario 6 (4.56 mm, 0.24%, and 2.94 mm) performed with similar accuracy. Scenario 2 (9.29 mm, 0.53%, and 4.55 mm) performed with the least amount of accuracy. Figure 5 shows the percent differences for the middle side sample distances.

For the right side, Scenario 3 (1.49 mm, 0.24%, and 0.61 mm) performed with the highest level of accuracy; Scenario 1 (4.13 mm, 0.66%, and 1.30 mm) was the next best; Scenario 4 (4.47 mm, 0.72%, and 1.44 mm) was the third most accurate, then Scenario 5 (4.84 mm, 0.78%, and 1.54 mm) and Scenario 6 (4.86 mm, 0.78%, and 1.54 mm) which performed similarly, and lastly Scenario 2 (6.26 mm, 1.01%, and 1.90 mm) performed with the least amount of accuracy. Figure 6 displays the percent differences for the right side sample distances.

Overall, Scenario 1 performed with the highest amount of accuracy (3.72 mm, 0.33%, and 1.89 mm) and then Scenario 6 (5.69 mm, 0.49%, and 2.73 mm) and Scenario 5 (5.69 mm, 0.49%, and 2.74 mm). The prevailing patterns that we saw throughout this model were Scenario 2 performed best on the left side, Scenario 3 performed best on the right side, Scenario 5 and 6 had nearly identical results, and on average Scenario 1 performed had the best results.

Object 3: Storage Building. The storage building model was the only full object model completed in our research. The six scale bar scenarios were carried out on each of the four sides and twenty-four sample distances were selected to be used for the comparison (six on each exterior wall).

Overall, Scenario 3 performed with the highest level of accuracy which had an average absolute difference value of 1.63 m, an average percent difference value of 0.18%, and a standard deviation of 1.37 mm. Scenario 2 (1.67 mm, 0.18%, and 1.43 mm) was the second most accurate, then Scenario 1 (1.89 mm, 0.20%, and 1.78 mm), Scenario 5 (2.07 mm, 0.24%, and 1.71 mm), Scenario 6 (2.09 mm, 0.24%, and 1.60 mm), and lastly Scenario 4 (2.09 mm, 0.24%, and 1.60 mm). This result is surprising because Scenarios 1-3 outperformed Scenarios 4-6 which have more scale bars referenced. There are similar patterns that were already observed in the previous two models: 1) Scenario 2 generally performed better for sample distances on the left side of each wall (where its scale bar was referenced) and Scenario 3 performed better for sample distances on the right side of each wall, 2) Scenario 5 and Scenario

6 performed with similar results. Figure 7 is a scatter plot of the percent differences. The scatter plot is grouped by scenario to display how the scenarios performed over the whole model.

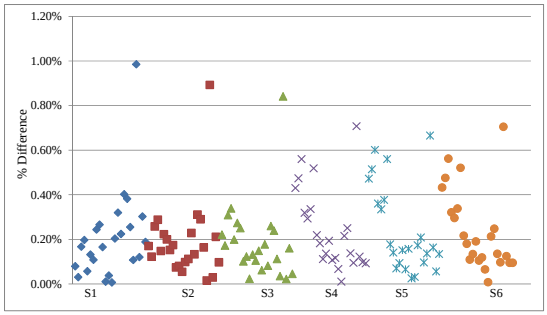

Figure 7. % Differences by scenario

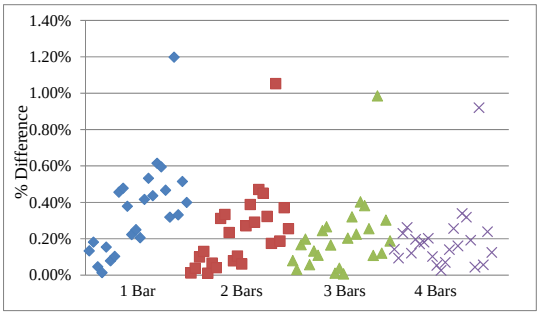

Figure 8. % Differences by quantity

The other data analysis that we carried out on this model was a quantity comparison. Instead of arranging the scale bars in the six scenarios, one scale bar was referenced in the middle of each wall of the building (in other words, four total scale bars) and the sample distance values were obtained on the model. To compare the effect of the quantity of total scale bars, we decreased the number of scale bars by increments of one and recorded the sample distance values.

As expected, the trial with four total scale bars referenced performed with the greatest amount of accuracy having an average absolute distance of 1.72 mm, an average percent difference of 0.19%, and a standard deviation of 1.50. The trial with three total scale bars referenced performed with the next best results (1.89 mm, 0.20%, and 1.78), two total scale bars performed with the next best results (2.24 mm, 0.24%, and 2.05), and lastly one total scale bar performed with the worst results (3.39 mm, 0.35%, and 2.48). Figure 8 shows a scatter plot of the percent difference values that are arranged by trial.

DISCUSSION AND CONCLUSION

One thing to keep in mind is that all of these models were produced under nearly ideal conditions (pictures were taken from approximately 1.5 meters away, the zoom was at the lowest setting, lighting was nearly ideal, etc.), so producing similar accuracy levels in a real-world application is unlikely. However, the results obtained in our research are still valid for drawing conclusions on scale bar quantity and placement.

There were three prevailing patterns that surfaced throughout: 1) Scenario 1 performed with consistent accuracy results for all sample distance locations (left, middle, right), 2) Scenario 2 was more accurate for distances located on the left side of the model (where its scale bar is referenced) and Scenario 3 was more accurate for distances located on the right side of the model, and 3) Scenarios 5 and 6 performed with similar accuracy results while Scenario 4 performed slightly less accurately in comparison. These results are fairly intuitive and didn't come to large extent as a surprise to our experimental expectations. However, we did observe that area of

interest where a measurement is planned really plays a role when we decide the scale bar placement.

For the most consistent results with one reference line, we would suggest referencing it horizontally in the middle of the selected object. If there is a particular area on your object that needs to be modeled more accurately than others, then it would be a good practice to place a reference line in that area also. As far as quantity is concerned, there was a leveling off of accuracy benefit that happened from three scale bars to four scale bars, so we suggest that two or three scale bars be referenced on the selected object for the best results.

ACKNOWLEDGEMENTS

The authors acknowledge NASA WV EPSCoR for its partial support.

REFERENCES

Brilakis, I., Fathi, H., and Rashidi, A. (2011). "Progressive 3D reconstruction of infrastructure with videogrammetry." *Autom. Constr.*, 20(7), 884 -895.

Dai, F., and Lu, M. (2010). "Assessing the accuracy of applying photogrammetry to take geometric measurements on building products." *Journal of Construction Engineering and Management*, 136(2), 242-250.

Dai, F., and Lu, M. (2008). "Photo-based 3D modeling of construction resources for visualization of operations simulation: case of modeling a precast facade." *Proceedings of the 2008 Winter Simulation Conference*, 2439-2446.

Fraser, C. (1997). "Digital camera self-calibration." *Journal of Photogrammetry and Remote Sensing*. 52(4): 149-159.

Grussenmeyer, P., and Al Khalil, O. (2002). "Solutions for exterior orientation in photogrammetry: a review." *The Photogrammetric Record*, 17(100), 615–634.

Kim, H., and Kano, N. (2008). "Comparison of construction photograph and VR image in construction progress." *Autom. Constr.*, 17(2), 137-143.

Shufelt, J. (1996). "Exploiting photogrammetric methods for building extraction in aerial images." *International Archives of Photogrammetry and Remote Sensing*. XXXI, B6, 74-79.

Smith, M., and Park, D. (2000). "Absolute and exterior orientation using linear features." *International Archives of Photogrammetry and Remote Sensing. XXXIII*, B3, 850-856.

Wegmann, H. (2002). "Image orientation by combined (A)AT with GPS and IMU." *ISPRS Com. I, Midterm Symposium, Integrated Remote Sensing at the Global, Regional, and Local Scale*, Denver, U.S.A., 10-15 November 2002.

Wolf, P. (1983). *Elements of photogrammetry*, McGraw-Hill, New York.